STRENGTH
AND PLASTICITY

Transformation of the Structure and Parameters of Phases during Aging of a Titanium Ti−10V−2Fe−3Al Alloy and Their Relation to Strengthening

A. V. Zhelnina[a], *, M. S. Kalienko[a, b], A. G. Illarionov[b, c], and N. V. Shchetnikov[a]

[a]*PAO Corporation VSMPO-AVISMA, Verkhnyaya Salda, 624760 Russia*
[b]*Ural Federal University n.a. the First President of Russia B.N. Yeltsin, Institute of Natural Sciences and Mathematics, Ekaterinburg, 620002 Russia*
[c]*Mikheev Institute of Metal Physics, Ural Branch, Russian Academy of Sciences, Ekaterinburg, 620108 Russia*
*e-mail: illarionovag@mail.ru

Abstract—Scanning electron microscopy, electron microprobe and X-ray diffraction analyses, and durometry are used to study changes in the structure, phase composition, and hardness of a quenched titanium Ti−10V−2Fe−3Al alloy in the course of aging at 500°C for 2−32 h. A complex analysis of changes in the lattice parameters of the primary and secondary α phases formed in the alloy during aging has been performed for the first time using full-profile X-ray diffraction analysis. Aging-induced changes in the hardness of the alloy are shown to be determined both by the sizes of formed secondary α-phase particles and changes in the alloying of the matrix β solid solution.

INTRODUCTION

High-strength titanium alloys based on the β phase, including the Ti−10V−2Fe−3Al alloy (hereinafter, the Ti−10−2−3 alloy), owing to the combination of high specific and fatigue strength, fracture toughness, hardenability, etc., are the base structural aircraft materials for manufacturing high-loaded elements of airframe and underframe units [1]. The complex of the properties of the Ti-10-2-3 alloy is formed in the course of quenching within the (α + β) region and subsequent aging (strengthening heat treatment (SHT)) or thermomechanical treatments related to decomposition processes of a metastable β solid solution [1−6]. In this case, the properties of the alloy are quite sensitive to variations of the chemical composition of the alloy within the grade and SHT conditions, which determine characteristic changes occurring during aging [1, 6]. The diffusion redistribution of alloying elements between the α and β phases is therefore of interest. This occurs in the course of decomposition of metastable β phase of the solid solution during aging of the alloy.

It is known [7] that the alloying elements have different maximum solubilities in each of the phases. The α stabilizer Al is the component of the alloy which exhibits high solubility in the α solid solution, and V

and Fe, which are β stabilizers, dissolve (themselves) mainly in the β matrix. The concentration of alloying elements in the phases also depends on the preparation method of structural and phase states [8]. However, we failed to find the complex analysis of regularities of these changes occurring during aging of the Ti−10−2−3 alloy. The redistribution of alloying elements between the phases, which occurs during aging, determines the physical-mechanical properties of structural elements, affects the level of strengthening of the α and β phases, critical stresses for the onset of plastic deformation, and permeability of interphase boundaries [9−11]. The study of the aforementioned phenomena helps to clarify the regularities of transformations which occurred in the (α + β) titanium alloys during heat treatment and to find their interrelation with the complex of mechanical properties. It should be noted that the direct determination of the concentration of alloying elements with a high locality, which is comparable with the typical sizes of secondary α-phase precipitates (30−60 nm), is rather difficult and requires expensive equipment, for example, an atomic-force scanner or a transmission electron microscope equipped with special analytical attachments [12, 13]. However, widely accessible X-ray diffraction analysis also allows one to analyze qualitatively and, in a number of cases, quantitatively, the
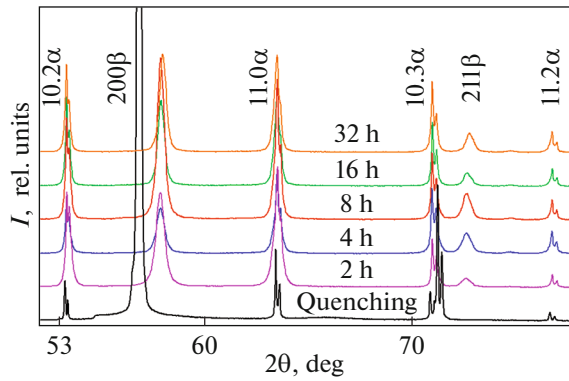
Fig. 1. X-ray diffraction patterns of the Ti−10−2−3 taken after SHT.

Fig. 2. (a) Structure of the quenched Ti−10−2−3 alloy and (b) variations in the chemical compositions of the phases.

dynamics of diffusion processes using changes in lattice parameters of the phases [5]. Based on the aforesaid, the aim is to analyze changes in the structure and phase composition of the quenched Ti−10−2−3 alloy, which include the evolution of lattice parameters and alloying of phases and their effect on the strengthening during aging of the alloy.

EXPERIMENTAL

We used a rod 20 mm in diameter as the material for the investigation, which was prepared from the Ti−9.3V−1.8Fe−3.0Al alloy (wt %) subjected to hot deformation in the ($\alpha + \beta$) region; the rod was manufactured at the PAO Corporation VSMPO-AVISMA. The rod was subjected to SHT, which consists of water quenching from the ($\alpha + \beta$) region from the heating temperature equal to 753°C and subsequent aging at 500°C with holdings for 2, 4, 8, 16, and 32 h.

The analysis of the microstructure and local chemical composition of heat-treated samples was performed by scanning electron microscopy (SEM) using a Quanta 3D FEG electron microscope equipped with an EDAX Genesis 2000 electron microprobe analyzer and a back-scattered electron diffraction (BSED) detector; microsections of longitudinal section of rod were analyzed. X-ray diffraction (XRD) analysis which included the calculation of lattice parameters of identified phases was performed in the angular range $2\Theta = 34°−105°$ at a step of 0.02° and 1-s exposition per point using a Bruker D8 Advance diffractometer equipped with a LynxEye detector and Cu$K\alpha$ radiation. The full-profile analysis of taken X-ray diffraction patterns was performed using TOPAS 3 software [14] and the refined parameters of model, which is used for profile function fitting and consists of three phases, such as two α phases, namely, the primary (α_I) and secondary (α_{II}) phases with an hcp lattice and the matrix β phase with a bcc lattice. The Vickers hardness of quenched and aged samples was measured at a load of 9.8 N using a DuraScan50 tester.
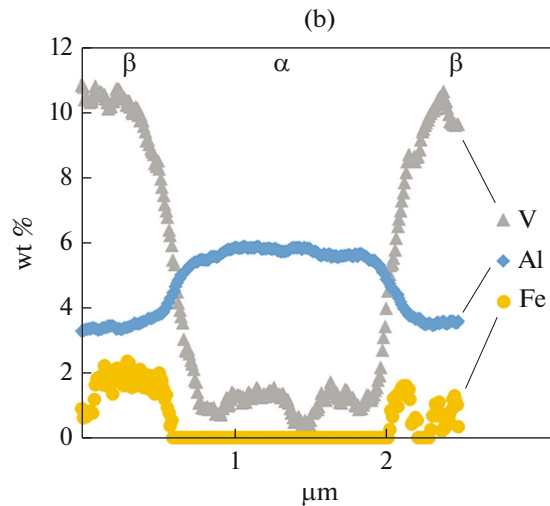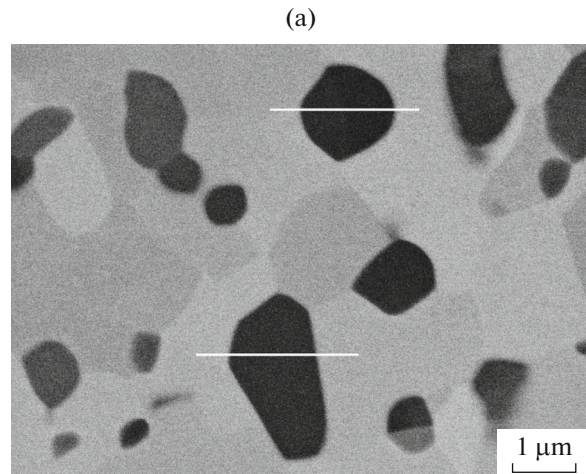
RESULTS AND DISCUSSION

X-ray diffraction patterns taken from the quenched alloy (Fig. 1) indicate intense reflections of the matrix β and primary α_I phases, whose lattice parameters are $a_\beta = 3.2410$ Å and $a_{\alpha I} = 2.93201$ Å and $c_{\alpha I} = 4.67843$ Å, ($c/a_{\alpha I} = 1.5956$), respectively.

The reflections of the α_I phase are characterized by splitting into the $K_{\alpha 1}−K_{\alpha 2}$ doublet (Fig. 1) that is usually recorded at the minimum density of dislocations in the phase [15] and, in the present case, is related to the occurrence of spheroidization and recrystallization processes in the course of heating and holding at the quenching temperature.

The analysis of the structure of the quenched alloy (Fig. 2a) showed that the primary α_I phase precipitates are indeed present in the form of globules 2−3 μm in size and are arranged mainly at β-phase subgrain boundaries.
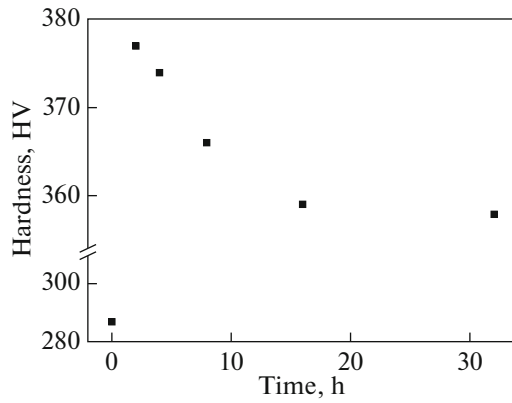
Fig. 3. Hardness of the Ti−10−2−3 alloy subjected to quenching and aging at 500°C.

It should be noted that no α″ martensite was found in the quenched Ti−10−2−3 alloy, which often forms upon water cooling [2, 16]. This is likely to be related to the fact that the alloying of the β solid solution upon quenching from the two-phase (α + β) region ensures the decrease in the temperature of the onset of martensite transformation (M_s) below room temperature.

The estimation of the M_s temperature by formula [17] $M_s = T_{pt} − 80Mo_{eq} − 7Al_{eq}$, where T_{pt} is the (α + β) − β polymorphous transformation temperature of the alloy (in this case, it was determined by the trial quenching method and is 798°C) and Mo_{eq} and Al_{eq} are the so-called molybdenum and aluminum equivalents of the alloy [1], which take into account, with certain coefficients, the contents of β and α stabilizers in the alloy, respectively. Taking into account the average chemical composition of the β phase at the quenching temperature (wt %) Ti−10.967V−2.12Fe−2.86Al, which was calculated using JMatPro software, we obtain the temperature:

$$M_s = 798 − 80 \times (10.97\% \, V / 1.4 + 2.12\% \, Fe \times 2)$$
$$− 7 \times 2.86\% \, Al = −192.5°C,$$

which is below room temperature.

The hardness of the alloy quenched from the (α + β) region is 287 ± 2 HV (Fig. 3). It is higher than that given in [5, 18] (260−275 HV), which was obtained after quenching from the β-phase region. In our case, the higher hardness of the alloy is related to the fixation of fine β-phase subgrains ~4 μm in size (150 μm obtained in [5]) because of the deceleration of grain growth by $α_I$-phase particles, which was not found in [5, 18].

Figures 4a, 4b show the structure of the aged Ti−10−2−3 alloy. In contrast to the quenched state, the aged state is characterized by fine plate-like $α_{II}$-phase precipitates formed along with the $α_I$ phase, which are fixed in the β matrix and tend to growth with increasing aging time.

The precipitation of the $α_{II}$ phase during aging favors the precipitation-strengthening of the alloy and ensures for it to have higher hardness compared to the hardness for the quenched alloy (Fig. 3). At the same time, as the aging time increases from 2 to 32 h, the hardness of the alloy decreases (Fig. 3). The decrease was also observed in [3] and, in our case, is related to the coarsening of $α_{II}$-phase particles (Figs. 4a, 4b) noted above.

X-ray diffraction patterns of the aged alloys exhibit the overlapping of reflections of the $α_I$ and $α_{II}$ phases (Fig. 1). To resolve the reflections, we used full-profile analysis. Figure 5 shows X-ray diffraction patterns of the aged samples, in which the $α_I$- and $α_{II}$-phase reflections simulated by full-profile analysis are also shown.

The full-profile analysis of the alloy aged for 32 h allowed us to fix the splitting of diffraction reflections of the $α_{II}$ phase into the $K_{α1} − K_{α2}$ doublet. This allows us to reach the threshold level of crystallite size, at which the size factor stops making a substantial contribution to the reflection broadening [19]. The X-ray diffraction data were used to calculate the aging-induced change in the coherent domain (CD) size of the $α_{II}$ phase, which directly is related to its sizes [20]. The CD of the $α_{II}$ phase and, therefore, the phase precipitate size increase as the aging time increases (Fig. 6a); this agrees with data on the microstructure (Figs. 4a, 4b).

As the aging time increases, changes in the positions of diffraction maxima of the phases and, therefore, the lattice parameters of the α and β phases in the alloys, are observed (Figs. 6b−6d). As is known [8, 21], this is related to the redistribution of alloying substitutional elements (Al, V, and Fe) between the α and β phases [7, 10], which have a lower atomic size than that of titanium [22]. According to data of [22, 23], the parameter of the bcc lattice of the β phase depends on the Al, V, and Fe contents (at %) in the phase as follows:

$$a_β = 3.282 − (0.154\% \, Al − 0.236\% V$$
$$− 0.5445\% \, Fe) \times 10^{-2} \, (\text{Å}). \tag{1}$$

When Al, V, and Fe are dissolved in the α phase, the lattice parameters a and c decrease; however, aluminum increases the parameter c/a [22], whereas vanadium and iron decrease it [22−24].

An analysis of the obtained dependences of the lattice parameters and unit-cell volumes of crystal lattices of the $α_I$, $α_{II}$, and β phases on the aging time (Fig. 5) showed that, as the aging time increases from 2 to 32 h, a decrease in the lattice parameters $a_β$, $a_{αI}$, $c_{αI}$, $(c/a)_{αI}$, $V_β$, and $V_{αI}$, an increase in the lattice parameters $a_{αII}$, $c_{αII}$, and $V_{αII}$, and little change in the parameter $(c/a)_{αII}$ are all observed. The decrease in the lattice parameter $a_β$ and, therefore, the unit-cell
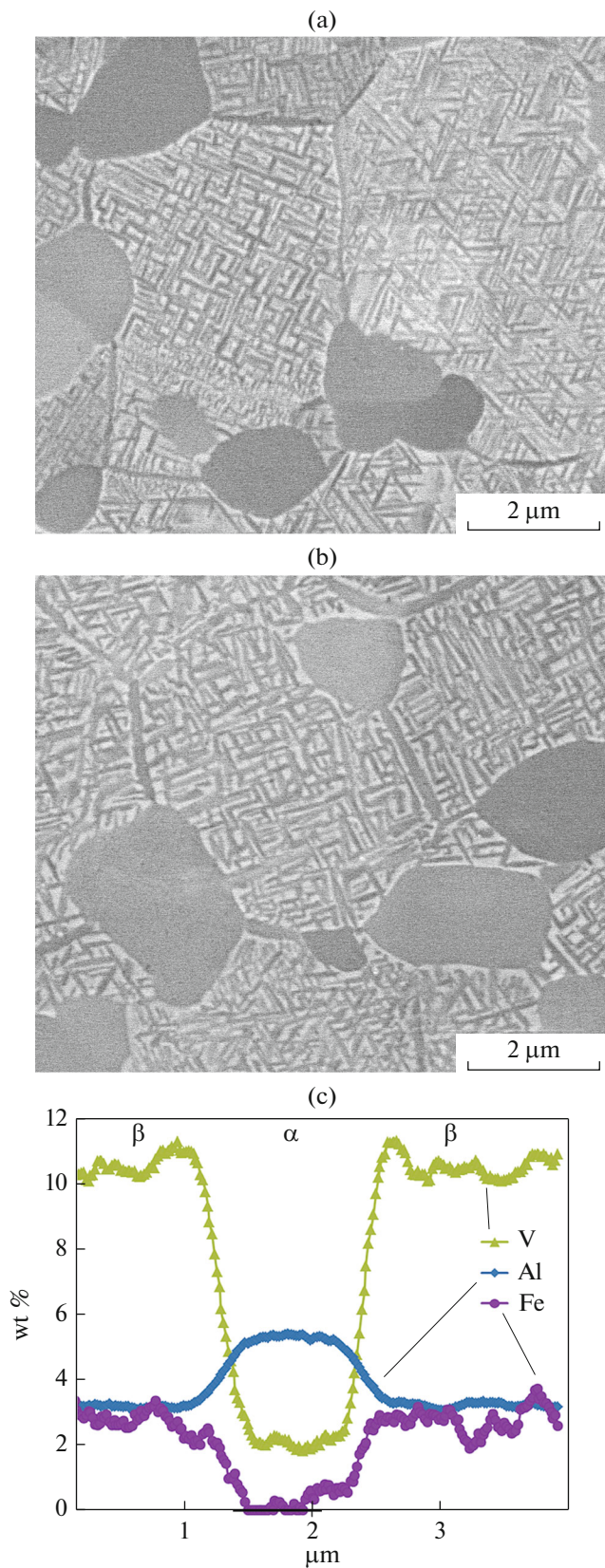
(a)

(b)

(c)

Fig. 4. Structure of the Ti−10−2−3 alloy aged at for (a) 2 and (b) 32 h and (c) variations of the chemical composition of the phases after aging for 32 h.
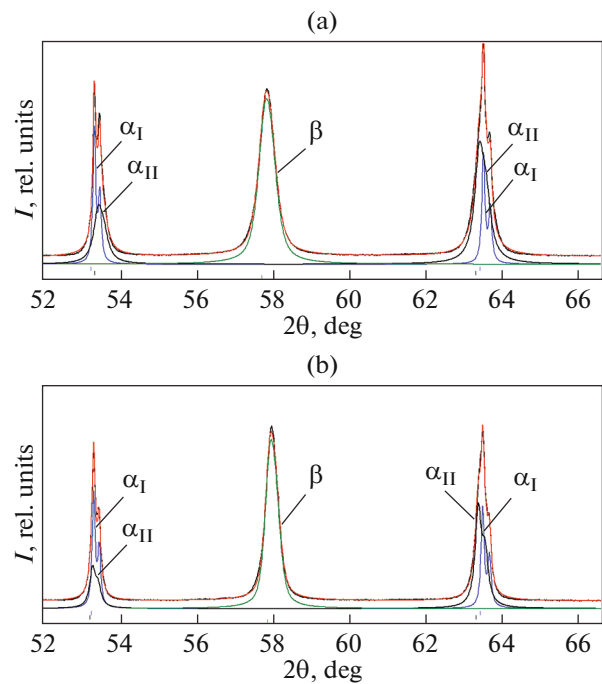
(a)

(b)

Fig. 5. Full-profile analysis of X-ray diffraction patterns of the alloy aged for (a) 2 and (b) 32 h.

volume V_β is caused by the enrichment of the β phase in β stabilizers, namely, vanadium and iron as a result of their transition into the β solid solution from the α_{II} phase, which forms during aging and is depleted of these elements; as the aging time increases, the depletion increases at the expense of the formation of the more coarse and, therefore, more equilibrium precipitates with the lower contents of β stabilizers. As the aging time increases, the progressive decrease in the vanadium and iron contents in the α_{II} phase ensures the regular increase in the lattice parameters $a_{\alpha II}$ and $c_{\alpha II}$ and unit-cell volume $V_{\alpha II}$, since the α_{II} phase is depleted of the elements (V, Fe) with the minimum atomic radius. The almost unchanged parameter $(c/a)_{\alpha II}$ observed in the course of aging is likely to be related to the close rates of increase in the lattice parameters $a_{\alpha II}$ and $c_{\alpha II}$ as a result of changing the phase alloying.

The slight decrease in all parameters of the α_I phase ($a_{\alpha I}$, $c_{\alpha I}$, $c/a_{\alpha I}$, and $V_{\alpha I}$) is explained by its progressive enrichment in vanadium and iron along with the slight decrease in the aluminum content in the course of aging compared to the content for the quenched state (Figs. 2b and 4c).

On the whole, as the aging time increases, the lattice parameters of the α_I and α_{II} phases vary in opposite directions, i.e., the lattice parameters of the α_I phase decrease, whereas the lattice parameters of the α_{II} increases. The cause for this consists in the different composition of phases which participate in the transformation of the α_I and α_{II} phases during aging.
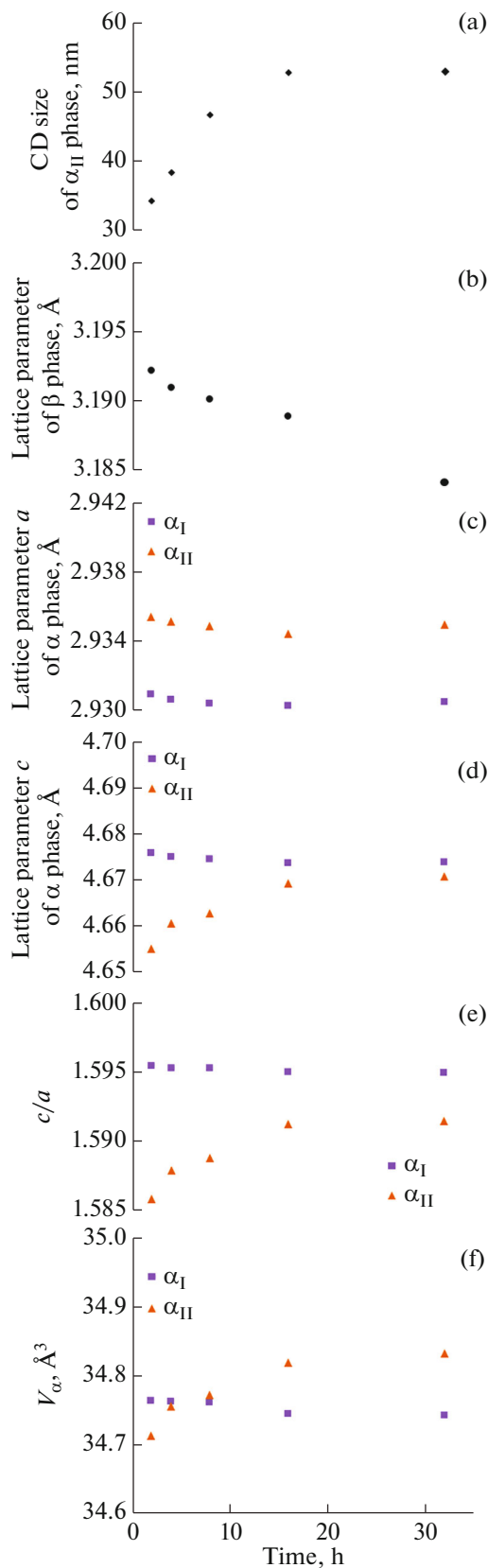
Fig. 6. Lattices parameters of the (a, c–f) α and (b) β phases in the Ti−10−2−3 alloy as a function of aging time.

For the α_I phase, the phase is itself the α_I phase which, after aging, is enriched in aluminum and depleted of vanadium and iron with respect to their contents for the aged state; for the α_{II} phase, the phase is the matrix β solid solution which, with respect to the α_{II} phase, is enriched in vanadium and iron and is depleted of aluminum. An interesting result related to this is the fact that, after aging for more than 10 h (Fig. 6f), the unit-cell volume $V_{\alpha II}$ was found to be higher than the unit-cell volume $V_{\alpha I}$, although after shorter aging, the inverse relation ($V_{\alpha I} > V_{\alpha II}$) occurs. It can be concluded, that during aging at holdings more than 10 h, the content of alloying elements in the α_{II} phase is lower than that in the α_I phase; at the initial stages of aging, the inverse relation was observed. In our opinion, this effect is related to the different sizes of the α_I- and α_{II}-phase precipitates (Fig. 2). The size of α_I-phase precipitates is higher than that of the α_{II} phase by two orders of magnitude, and the equalizing of the composition of the α_I phase to a state close to the equilibrium one is substantially slower than that of the α_{II} phase, since, as is known [25], the diffusion path of an element at a fixed temperature is proportional to the square root of the holding time at this temperature.

As was noted above (Fig. 3), during aging, the increase in durometic characteristics is observed, which can be related to the precipitation of fine α_{II}-phase particles. The strengthening effect decreases after prolonged holdings; one of the causes is coarsening the α_{II}-phase particles (Figs. 4a, 4b). The estimation of the strengthening at the expense of growth of α_{II}-phase particles upon aging shows that, when only the precipitation strengthening is taken into account, the decrease in the hardness should be higher than that observed experimentally. In particular, after 2-h aging, the difference in the hardness of aged and quenched state, i.e., the strengthening is 89 HV (377−288), whereas after 32-h aging, the difference is 70 HV (358−288). At the same time, according to XRD data (Fig. 6a) on the CD size related to the α_{II}-phase particle size, the increase in the aging time from 2 to 32 h leads to an increase in the CD size by 1.56 times (53 nm/34 nm). As is known [25], the effect of precipitation strengthening is inverse to the size of precipitated particles ($\tau \approx Gb\sqrt{f}/r$, where τ is the critical shear stress; G is the shear modulus of the β matrix; b is the abs.value of Burgers vector for the β matrix; f is the volume fraction of α_{II}-phase particles; and r is the α_{II}-hphase particle size). According to data of [2], the minimum used time of aging at 500°C, 2 h, exceeds the time of the arbitrary end of the decomposition in the Ti−10−2−3 alloy; because of this the volume fraction (f) of α_{II}-phase particles is almost unchanged for a holding time range of 2−32 h. The parameters G and b will have close values. It follows that the τ value mainly is affected by the parameter r, i.e., the α_{II}-phase particle

size. Because of this, when the strengthening effect is related to only the dispersivity of α_{II}-phase particles, the value of strengthening after aging should not exceed 57 HV (89 HV/1.56); however, the value was found to be 70 HV, i.e., by 13 units higher. Thus, along with the precipitation strengthening with increasing aging time, the additional strengthening occurs in the alloy, which, according to data of [18], may be related to the solid-solution strengthening of the β matrix as a result of its abovementioned enrichment in vanadium and iron during aging. Let us estimate the possible order of such a strengthening, taking into account changes in the lattice parameter of the β phase.

As was noted above, using the content of alloying elements Al, Fe, and V, the lattice parameter of the β phase in the Ti−10−2−3 alloy can be determined by Eq. (1). To estimate the equilibrium aluminum, vanadium, and iron contents in the α and β phases in the alloy under study at an aging temperature of 500°C, the calculations were performed using JMatPro software (Table 1).

The calculated content of alloying elements in the β phase at 500°C agrees well with that determined experimentally for the alloy in [26] at 500°C, namely, Ti−2Al−16V−6.4Fe. The vanadium content is the exception; according to calculations, the vanadium content in the β phase at 500°C should be two times higher as compared to that obtained in [26]. At the same time, according to the obtained EMA data (Fig. 4c), the vanadium content in the α_I phase after aging is ~1.8%; taking into account the data given in Fig. 6f, the vanadium content in the α_{II} phase is even lower. According to data of [16], the volume fraction of the β phase in the alloy at 500°C is ~30%. In this case, the calculation shows that, at a vanadium content in the alloy of 9.3%, the vanadium content in the β matrix should be no less than 25% (9.3−1.8)/0.3. Within the 20% error, it is comparable with the calculated data.

According to the calculations, as compared to the average chemical composition of the alloy, the vanadium and iron contents in the β phase after aging vary more substantially (by three times and more); the aluminum content varies less substantially (no more than by 1.5 times). Moreover, taking into account the factors in Eq. (1), aluminum makes the smallest contribution to the change in the lattice parameter of the β phase. The conversion of the calculated vanadium and iron contents in the alloy into atomic percentages shows that, at 500°C, the calculated ratio %V/%Fe is 5.28/1. Because of this, to simplify the calculations, we assume that as the aging time increases, the aluminum content in the β phase is unchanged, and the calculations are performed initially using only the arbitrary ion content. Making such assumptions, we estimate changes in the vanadium and iron contents in the

Table 1 Calculated equilibrium contents of alloying elements in the α and β phases in the Ti−10−2−3 alloy (wt %) at 500°C

Phase	V	Fe	Al
$\alpha_{I,II}$	1.35	0.02	3.38
β	31.12	6.46	1.99

β phase as the aging time increases from 2 to 32 h by the following formula:

$$\Delta a = a_{32} - a_2 = -0.236\Delta V - 0.5445\Delta Fe$$
$$= -0.236\Delta Fe \times 5.28 - 0.5445\Delta Fe = -1.7245\Delta Fe.$$

We obtain $\Delta a = -0.84$ nm; in this case, $\Delta Fe = 0.487$ at % (0.575 wt %), $\Delta V = 5.28\Delta Fe = 2.572$ at % (2.77 wt %).

As a result of the enrichment of the β matrix with vanadium and iron with increasing aging time from 2 to 32 h, the strength molybdenum equivalent [27] of the β solid solution increases by $\Delta Mo = 2.77\%V/1.7 + 0.575\%Fe/0.7 = 2.45$; this makes a contribution to the increase in the strength $\Delta\sigma = 50\Delta Mo = 50 \times 2.45 = 122.5$ MPa. For titanium alloys, the following correlation between σ and H_V is available [7, 18]: $\sigma = 9.81/3 \times H_V$; from this correlation, $\Delta H_V = 3\Delta\sigma/9.81$. Taking into account the volume fraction of β phase in the structure ($\approx 30\%$), the calculated increase in the hardness is $\Delta H_V = (3 \times 122.5 \text{ MPa}/9.81 \text{m/s}^2) \times 0.3 = 11$ HV. The performed calculation of the solid solution strengthening of the β phase at the expense of its enrichment in the vanadium and iron with increasing aging time gives the value 11 HV, which within the 15% error gives the required 13 HV, in order to compensate the softening at the expense of α_{II}-phase particle growth.

CONCLUSIONS

(1) The phase state of the Ti−10−2−3 alloy, which is fixed by quenching, is determined by the distribution of alloying elements in the β and α_I phases and is characterized by higher hardness compared to that available in the literature for the quenching from the β-phase region.

(2) The aging of the alloy at 500°C for 2−32 h leads to the precipitation of disperse α_{II}-phase particles from the β matrix, which tend to growth as the holding time increases.

(3) As the holding time during aging increases, the strengthening of the alloy is shown to depend on at least two factors; these are the precipitation strengthening at the expense of the α_{II} phase, the level of which decreases because of the increase in the phase precipitate sizes, and the solid solution strengthening of the β matrix, which increases at the expense of its enrichment in vanadium and iron.

(4) The redistribution of alloying elements (Al, V, and Fe) between the β, α_I, and α_{II} phase in the course of aging is found to ensure regular changes in the lattice parameters of these structural components.

REFERENCES

1. J. D. Cotton, R. D. Briggs, R. R. Boyer, S. Tamiri-sakandala, P. Russo, N. Shchetnikov, and J. C. Fanning, "State of the art in beta titanium alloys for airframe applications," JOM **67**, No. 6, 1281−1303 (2015).

2. T. W. Duerig, G. T. Terlinde, and J. C. Williams, "Phase transformations and tensile properties of Ti−10V−2Fe−3Al," Metall. Trans. A **11**, 1980−1987 (1980).

3. A. G. Illarionov, A. V. Korelin, A. A. Popov, S. M. Illarionova, and O. A. Elkina, "Formation of the structure, phase composition, and properties in high-strength titanium alloy upon isothermal and thermomechanical treatment," Phys. Met. Metallogr. **119**, No. 8, 780−788 (2018).

4. O. P. Shaboldo, Ya. M. Vitorskii, V. V. Sagaradze, N. L. Pecherkina, and M. A. Skotnikova, "Formation of the structure and properties of β-type titanium alloy upon thermomechanical treatment," Phys. Met. Metallogr. **118**, No. 1, 75−80 (2017).

5. A. G. Illarionov, A. V. Trubochkin, A. M. Shalaev, S. M. Illarionova, and A. A. Popov, "Effect of microalloying, with rem inclusively, on the structure, phase composition and properties of (α + β)-titanium alloy," Met. Sci. Heat Treat. **57**, 719−725 (2016).

6. R. R. Boyer and G. W. Kuhlman, "Processing properties relationships of Ti−10V−2Fe−3Al," J. Metall. Trans. A **18**, 2095−2103 (1987).

7. E. W. Collings, *The Physical Metallurgy of Titanium Alloys* (Park, Ohio, 1984), p. 261.

8. T. Li, M. Ahmed, G. ShiR. Sha, G. Casillas, H.-W. Yen, Y. Wang, E. V. Pereloma, and J. M. Cairney, "The influence of partitioning on the growth of intragranular α in near-β Ti alloys," J. Alloys Compd. **643**, 212−222 (2015).

9. C. Y. Wang, L. W. Yang, Y. W. Cui, and M. T. Pérez-Prado, "High throughput analysis of solute effects on the mechanical behavior and slip activity of beta titanium alloys," Mater. Des. **137**, 371−383 (2018).

10. C. Zou, J. Li, W. Y. Wang, Y. Zhang, B. Tang, H. Kou, H. Wang, J. Wang, D. Xu, and D. Lin, "Revealing the local lattice strains and strengthening mechanisms of Ti alloys," Comput. Mater. Sci. **152**, 169−177 (2018).

11. Y. Pan, Q. Sun, L. Xiao, X. Ding, and L. Juan, "Plastic deformation behavior and microscopic mechanism of metastable Ti−10V−2Fe−3Al alloy single crystal pillars orientated to ⟨011⟩β in submicron scales Part II: Phase transformation dependence of size effect and deformation mechanism," Mater. Sci. Eng., A **743**, 804−810 (2019).

12. B. Gault, M. P. Moody, S. P. Cairney, and S. P. Ringer, *Atom Probe Microscopy* (Springer Science & Business Media, 2012), p. 396.

13. D. B. Williams and C. B. Carter, *Transmission Electron Microscopy: Spectrometry. IV* (Plenum Press, New York, 1996), p. 610.

14. TOPAS. v3, General Profile and Structure Analysis Software for Powder Diffraction Data. User's manual. Karlsruhe, Germany: Bruker AXS, 2005.

15. I. C. Dragomir, D. S. Li, G. A. Castello-Branco, Snyder R. L. Garmestani, G. Ribarikd, and T. Ungar, "Evolution of dislocation density and character in hot rolled titanium determined by X-ray diffraction," Mater. Charact. **55**, 66−74 (2005).

16. P. Barriobero-Vita, G. Requena, F. Warchomicka, A. Stark, N. Shell, and T. Buslaps, "Phase transformation kinetics during continuous heating of a β-quenched Ti−10V−2Fe−3Al alloy," J. Mater. Sci. **50**, 1412−1426 (2015).

17. F. V. Vodolazskii, A. G. Illarionov, A. A. Popov, M. O. Leder, A. V. Zhloba, and A. V. Skidan, "A study of isothermal decomposition of β-solid solution in titanium alloy VST2," Met. Sci. Heat Treat. **57**, 458−462 (2015).

18. P. Li, T. SunX. Zhang, H. Zhang, D. Wang, Q. Sun, L. Xiao, and J. Sun, "Secondary hardening behavior in Ti alloy," Mater. Sci. Eng., A **759**, 640−647 (2019).

19. V. Uvarov and I. Popov, "Metrological characterization of X-ray diffraction methods at different acquisition geometries for determination of crystallite size in nanoscale materials," Mater. Charact. **85**, 111−123 (2013).

20. M. S. Kalienko, A. V. Volkov, and A. V. Zhelnina, "Use of full-profile X-ray analysis for estimation of the dispersity of the secondary alpha phase in high-strength titanium alloys," Crystallogr. Rep. **65**, 412−416 (2020).

21. F. W. Chen, G. Xu, X. Y. Zhang, K-C. Zhou, and Y. Cui, "Effect of α morphology on the diffusional β ↔ α transformation in Ti−55531 during continuous heating: Dissection by dilatometer test, microstructure observation and calculation," J. Alloys Compd. **702**, 352−365 (2017).

22. U. Tsvikker, *Titanium and Its Alloys* (Mir, Moscow, 1979) [in Russian].

23. G. Shao, A. P. Miodownik, and P. Tsakiropoulos, "ω-phase formation in V−Al and Ti−Al−V alloys," Philos. Mag. A **71**, No. 6, 1389−1408 (1995).

24. A. Kilmametov, Yu. Ivanisenko, B. Straumal, A. A. Mazilkin, H. Hahn, A. S. Gomakova, M. J. Kriegel, O. B. Fabrichnaya, and D. Rafaia, "Transformations of α′ martensite in Ti−Fe alloys under high pressure torsion," Scr. Mater. **136**, 46−49 (2017).

25. G. Gottshtain, *Physicochemical Basics of Materials Science* (Binom, Moscow, 2014) [in Russian].

26. M. Ahmed, D. Wexler, G. Casillas, O. M. Ivasishin, and E. Peraloma, "The influence of β phase stability on deformation mode and compressive mechanical properties of Ti−10V−2Fe−3Al alloy," Acta Mater. **84**, 124−154 (2015).

27. A. Il'in, B. A. Kolachev, and I. S. Pol'kin, *Titanium Alloys. Composition, Structure, Properties. Handbook* (VILS, Moscow, 2009) [in Russian].

Translated by N. Kolchugina